JMEPEG (2015) 24:4182–4191
DOI: 10.1007/s11665-015-1710-z

Electrolytic Synthesis and Characterization of Electrocatalytic Ni-W Alloy

Liju Elias, Keith Scott, and A.Chitharanjan Hegde

(Submitted July 13, 2015; in revised form August 30, 2015; published online September 11, 2015)

Inspired by the more positive (about 0.38 V nobler) discharge potential of hydrogen on Ni-W alloy compared to that on both Ni and W, a Ni-W alloy has been developed electrolytically as an efficient electrode material for water electrolysis. The deposition conditions, for peak performance of the electrodeposits for hydrogen evolution reaction (HER) and oxygen evolution reaction (OER) in 1.0 M KOH medium have been optimized. Electrocatalytic activity of the coatings, deposited at different current densities (c.d.'s) for water splitting reactions of HER and OER was tested by cyclic voltammetry and chronopotentiometry. It was found that Ni-W alloys deposited, at 4.0 A/dm^2 (having about 12.49 wt.% W) and 1.0 A/dm^2 (having about 0.95 wt.% W) are good electrode materials as cathode (for HER) and anode (for OER), respectively. A dependency of the electrocatalytic activity for HER and OER with relative amount of Ni and W, in the deposit was found. The variation of electrocatalytic activity with W content showed the existence of a synergism between high-catalytic property of W (due to low hydrogen overvoltage) and Ni (having increased adsorption of OH$^-$ ions), for hydrogen (as cathode) and oxygen (as anode) evolution, respectively. Electrocatalytic activities of the coatings, developed at different c.d.'s were explained in the light of their phase structure, surface morphology, and chemical composition, confirmed by XRD, FESEM, and EDX analysis. The effect of c.d. on thickness, hardness, composition, HER, and OER was analyzed, and results were discussed with possible mechanisms.

Keywords electrocatalysis, HER and OER study, Ni-W alloy

1. Introduction

Ni-based alloys, in particular, binary Ni-W, Ni-Mo, Ni-P, or ternary Ni-W-P or Ni-Mo-P, have attracted much interest over the decades for their many applications in decorative finishing or as corrosion and wear-resistant materials (Ref 1). Many studies on electrodeposition of Ni-W alloys have been made using citrate and pyrophosphate baths, reasoned by their unique combination of good corrosion resistance, tribological, magnetic, and electrocatalytic behaviors (Ref 2). Sridhar et al. have reviewed the literature on electrodeposition of Ni-W alloys and studied the effect of Ni^{2+}, Cit^{3+}, bath additives, applied current density, and bath temperature on the Faradaic efficiency, W content, and properties of Ni-W alloys deposited on stationary working electrodes (Ref 3). It is well known that elements, such as W, Mo, Ge, P, etc., cannot be deposited alone from their aqueous solutions. However, they may readily be codeposited with Fe-group elements such as Fe, Co, and Ni. The term-induced codeposition was coined by Brenner in 1963 to describe a situation where, 'a metal that cannot be deposited alone from its aqueous solution is codeposited in the presence of another metal, forming an alloy' (Ref 4). It was applied first to describe the electroless deposition of Ni-P alloys, and later for electroplating of alloys of W and Mo with the Fe-group metals (Fe, Co and Ni). Several hypotheses have been advanced to explain the mechanism of the induced codeposition. Among them, the most favored hypothesis is ennobling of the deposition potential of tungsten by virtue of the formation of a solid solution or inter-metallic compound (Ref 5). According to which the codeposition of W is based on the assumption that the deposition potential of W is too negative (−0.51 V) to be attained in water solution. It was further assumed that the formation of a solid solution of W with the Fe-group metal involves a sufficient decrease of free energy to shift the deposition potential of W to more positive (more noble) potentials. This hypothesis is considered to be more acceptable, and referred to as the shift of the deposition potential.

On the other hand, electrochemical water splitting into hydrogen evolution reaction (HER) and oxygen evolution reaction (OER) in alkaline solution, using an effective electrocatalyst plays a growing role in the fabrication of alternative energy devices, required for clean and sustainable energy. Strong intrinsic catalytic activity, large surface area, stability of performance, and low cost are the required properties of a good electrode material to be used for HER and OER (Ref 6). It is desirable that catalysts should demonstrate low over potentials toward the reaction, along with reasonable current densities. Up to now, for the hydrogen side ($2H_2O + 2e^- \rightarrow H_2 + 2OH^-$, in alkaline media), platinum is the best catalyst showing high cathodic current densities at negligible over potential (Ref 7). Albeit platinum shows almost perfect behavior for the HER, the drawback lies in the comparatively low abundance and the thus resulting high price. Additionally, new structured Pt materials with high surface area have been reported recently by different approaches (Ref 8, 9). Contrarily, the OER ($4OH^- \rightarrow O_2 + 2e^- + 2H_2O$, in alkaline media) is more complicated

---

Liju Elias and **A. Chitharanjan Hegde**, Electrochemistry Research Lab, Department of Chemistry, National Institute of Technology Karnataka, Surathkal, Srinivasnagar, Mangalore 575 025, India; and **Keith Scott**, School of Chemical Engineering and Advanced Materials, Newcastle University, Newcastle upon Tyne, UK. Contact e-mail: acrhegde@gmail.com.

due to the high number of steps involved. As in the HER, the best catalysts for the OER consist of less abundant and expensive materials such as RuO_2 and IrO_2. Alternatives comprising more abundant and cheap materials as cobalt (Co) (Ref 10), nickel (Ni) (Ref 11), iron (Fe) (Ref 12), manganese (Mn) (Ref 13), and their alloys (Ni-Co, Ni-Fe, Ni-Mo), oxides (Ref 14), nitrides, and carbides have been subject of intense research due to their promising electrocatalytic properties. In this direction, Ni-based alloys are considered to be one of the most efficient non-noble electrocatalysts in alkaline solution. Moreover, modifications (i.e., alloying and doping) of Ni and nickel oxide-based materials can result in higher activity, both for HER and OER (Ref 15).

The literature on electroactive materials confirms that electrocatalytic activity of electrode materials can be increased considerably by insertion of foreign dopants into materials possessing high surface areas, or better electroactive sites. Keeping this in mind, many effective nanocrystalline electrocatalytic materials have been produced by means of electrodeposition, using many baths under different deposition conditions. The electrolytic method of synthesis of these materials has genuine advantages over other methods. It allows the convenience of producing the deposits of desired composition, porosity (large area surfaces), low temperature growth and the possibility to control film thickness, morphology and phase structure by adjusting the electrical parameters and the composition of electrolytes (Ref 16, 17). With this incentive, recently we have reported the development of electrocatalytic Fe-Ni coatings for water splitting reaction in alkaline medium (Ref 18). The deposition current density (c.d.) was used to tune the composition of the coating for HER and OER, taking the advantage of anomalous codeposition. In continuation of search for more efficient electrode material, a new Ni-W bath has been proposed by adding glycerol as additive, taking advantages of both electrocatalytic activity and induced codeposition of metals involved. Ni-W alloy coatings were deposited at different current densities and characterized. Stability and electrocatalytic behaviors of the coatings were tested in 1.0 M KOH medium by cyclic voltammetry (CV) and chronopotentiometry (CP) methods. The water splitting ability for HER and OER was analyzed in the light of surface morphology, composition, and phase structures of the deposits, supported by FESEM, EDS, and XRD analyses.

2. Experimental

Ni-W alloy deposits were electroplated from aqueous solutions having composition shown in Table 1. Here $NiSO_4 \cdot 6H_2O$ (0.08-0.01 M) and $Na_2WO_4 \cdot 2H_2O$ (0.12-0.15 M), as metal salts of electroactive species $C_6H_5Na_3O_7 \cdot 2H_2O$ (0.40-0.50 M) in conjunction with NH_4Cl, as complexing agent; and glycerol, as organic brightener were used. All reagents used were of LR grade (Merck, Mumbai, India), prepared in distilled water. The pH was measured using Systronics, μ pH Systems 362, and adjusted to a value of 8.5 through additions of H_2SO_4 and NH_4OH as required. A Hull cell was used to determine the chemical composition, and range of the cathodic current densities for galvanostatic deposition (Ref 19). All experiments were performed at room temperature, under constant agitation. The operating parameters arrived on by optimization are shown in Table 1.

The electrolytic synthesis of nanocrystalline Ni-W alloy coatings/deposit has been accomplished on copper substrate, using an electrolyte having optimal bath composition in a 200 mL capacity cubic cell (made of PVC material). A DC Power Analyzer (Agilent N6705A, USA) was used as power source for electrodeposition. Copper plates having (7.5 cm × 2.5 cm × 0.2 cm) dimension were polished metallurgically to get mirror finish, and then degreased using trichloroethylene as solvent. Anode and cathode were kept parallel 5 cm apart during deposition. All depositions were carried out on (2.5 × 2.5 cm^2) active surface area, keeping other part insulated by cellophane tape, at 303 K and pH 8.5 for 10 min to compare their relative performance. Prior to plating, polished substrate was electro-cleaned, and then pickled in 0.5 M HNO_3. After deposition, the coatings were rinsed with distilled water several times, dried in hot air, and then desiccated until further testing.

The electrocatalytic behavior of Ni-W coatings was studied by depositing them on one end of a copper rod (having the same specification as the copper plate) with 1 cm^2 cross-sectional area, using a specially designed three-electrode tubular glass assembly, as shown in Fig. 1. Ni-W alloy deposit, having different compositions, and hence electrocatalytic activity were developed, from the same bath by modulating the deposition c.d. Electrodeposited copper rod was used as working electrode, platinized platinum of area 1.0 cm^2, as counter electrode, and a saturated calomel electrode (SCE) as reference electrode (Fig. 1). Electrocatalytic performance was evaluated by measuring the amount of H_2 and O_2 gases liberated, respectively, at cathode and anode, using graduated gas collector as shown in Fig. 1. All potentials reported in the present study are with respect to SCE (1.23 V). Luggin's capillary with Agar-KCl salt bridge was used to compensate the error due to Ohmic resistance. Electrocatalytic activity of the coatings for water splitting reactions of HER and OER was evaluated in alkaline medium of 1.0 M KOH. Cyclic voltammetry (CV) and chronopotentiometry (CP) techniques were used to arrive at optimal c.d. to deposit Ni-W alloy coatings with maximum electrocatalytic activity, for HER and OER. CV

Table 1 Composition and operating parameters of proposed bath for electrodeposition of bright Ni-W alloy coatings

Bath composition	Composition (per liter)	Operating parameters
Nickel sulfate hexahydrate ($NiSO_4 \cdot 6H_2O$)	22.4 g	pH: 8.5
Sodium tungstate dihydrate ($Na_2WO_4 \cdot 2H_2O$)	46.07 g	Temperature:303 K
Tri-sodium citrate dihydrate ($Na_3C_6H_5O_7 \cdot 2H_2O$)	102.06 g	Anode: Nickel
Boric acid (H_3BO_3)	20.0 g	Current density range: 1.0-4.0 A/dm^2
Ammonium chloride (NH_4Cl)	36.15 g	…
Glycerol ($C_3H_8O_3$)	20.0 mL	…

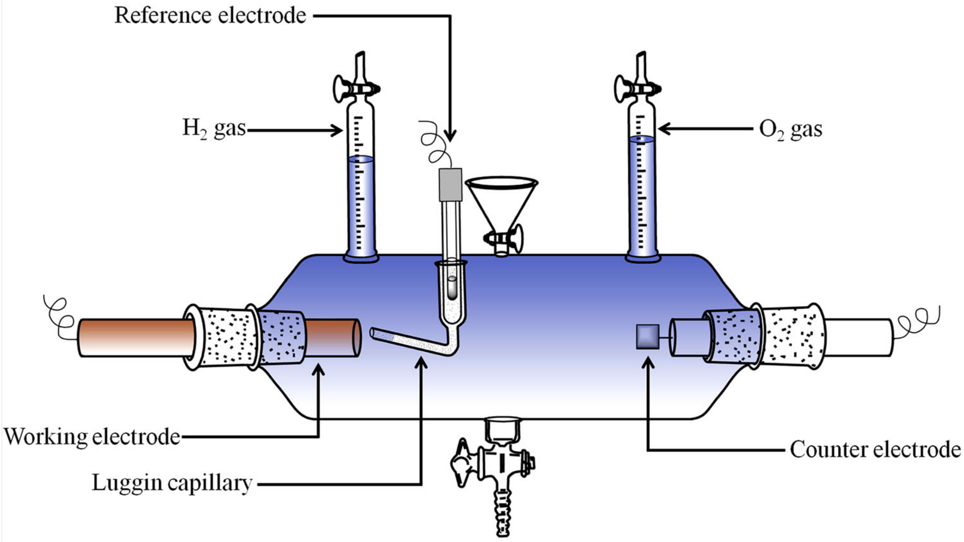

Fig. 1 Tubular three-electrode glass cell used for quantification of electrocatalytic behavior of Ni-W alloy deposit, in terms of H_2/O_2 gases liberated on electrode surface

and CP studies were carried out in the same three-electrode setup shown in Fig. 1.

Computer-controlled potentiostat/galvanostat (Biologic SP-150, Biologic Science Instruments, France) was used for all electrochemical catalytic studies. Corrosion stability of Ni-W alloy coatings was studied in 1.0 M KOH by potentiodynamic polarization (in potential range of ±250 mV around OCP, at a scan rate of 1 mV/s) and electrochemical impedance spectroscopy (EIS) (in the frequency range from 100 kHz to 10 mHz) methods. Electrodeposition of all Ni-W deposits was carried out galvanostatically for the same duration (600 s) for comparison purpose. The surface morphology of electrodeposited Ni-W coatings was analyzed using field emission scanning electron microscope (FESEM) (JSM-7610F from JEOL, USA). The composition of Ni-W coatings, deposited at different c.d.'s was evaluated by Energy dispersive x-ray spectroscopy (EDX) (Link ISIS-300 Micro-analytical System, Oxford Instruments, UK) interfaced with the FESEM machine. The change in the phases structure of Ni-W coatings with c.d. was analyzed by x-ray diffraction (XRD) study (JEOL JDX-8P0), using Cu Kλ (λ = 1.5406 Å) radiation, in continuous scan mode at a scan rate of 2°/min. The thicknesses of the coatings were calculated from Faradays law, and were verified using a Digital Thickness Tester (Coatmeasure M&C, ISO-17025). The hardness of the deposits was measured by Vickers method, using Micro Hardness Tester (CLEMEX, CMT. HD, Canada).

3. Results and Discussion

3.1 Induced Codeposition of Ni-W Alloy

Electrochemistry has a role in production of many functional materials at low cost and high degree of accuracy and reproducibility. The property of electrodeposited coatings can be tailored to a particular requirement by proper modulation of deposition conditions, like c.d., pH, temperature, etc. Furthermore, this study was inspired by the fact that the potential required for the discharge of hydrogen is about 0.38 V more noble (more positive) on Ni-W alloy than on either Ni or W, as individual metals. Hence Ni-W alloy is considered to be a promising material for HER applications. Though tungsten (W) is good replacement to less abundant and more expensive electro active materials, it cannot be deposited directly from its aqueous solutions and can be deposited only through induced codeposition. In the present study of induced codeposition of Ni-W alloy, the Fe-group metal (Ni) stimulates deposition and is called the *inducing metal*, and W, which does not deposit by itself, is called the *reluctant metal*. The effects of plating variables on compositions of the alloys of induced codeposition are more vagarious than in other types of alloy deposition (Ref 4). Particularly, with regard to the effect c.d., there is no consistent trend in the content of the reluctant metal in the deposit with c.d. Hence variations in properties of electrodeposited Ni-W alloy coatings with c.d. are quite unpredictable, and due to which the scope for studying the structure-property relationship of this alloy is very vast. Therefore, any study of Ni-W alloy deposition will be incomplete without discovering the effect of c.d. on its composition, phase structure, and surface morphology. Hence, the first part of this paper explains the deposition and characterization of Ni-W alloy deposited at different c.d.'s; and the second part details their electrocatalytic behavior as a function of their composition and phase structures.

3.2 Synthesis and Characterization of Ni-W Alloy

Conventional electrodeposition of Ni-W alloy coatings is generally carried out at c.d.'s in the range of 1.0-4.0 A/dm^2. A further increase of c.d., brings an increase in the wt.% W in the deposit, although it reduces the cathode current efficiency (CCE) of the bath due to excessive hydrogen evolution. Thus, low hydrogen overvoltage of the W alloy is probably the reason for the decrease in the cathode current efficiency of alloy deposition as the W content of the alloy increases. Hence, electrodeposition of Ni-W alloy coatings was confined to c.d.'s from 1.0 to 4.0 A/dm^2, using the optimal bath shown in Table 1. The deposits were found to be bright at all c.d.'s. The

Table 2 Composition, hardness, thickness, and corrosion data of Ni-W alloy coatings deposited from optimal bath at 303 K

c.d., A/dm^2	Wt.% of W in deposit	Micro hardness in Gpa (V_{100})	Thickness, µm	$-E_{corr}$ (mV vs. SCE)	i_{corr}, µA/cm^2	CR ($\times 10^{-2}$ mm/year)
1.0	0.95	2.520	8.3	287.1	9.06	7.3
2.0	4.36	2.687	10.5	349.1	6.94	5.6
3.0	8.34	2.834	12.4	380.6	5.45	4.4
4.0	12.49	3.152	15.9	398.1	2.14	1.6

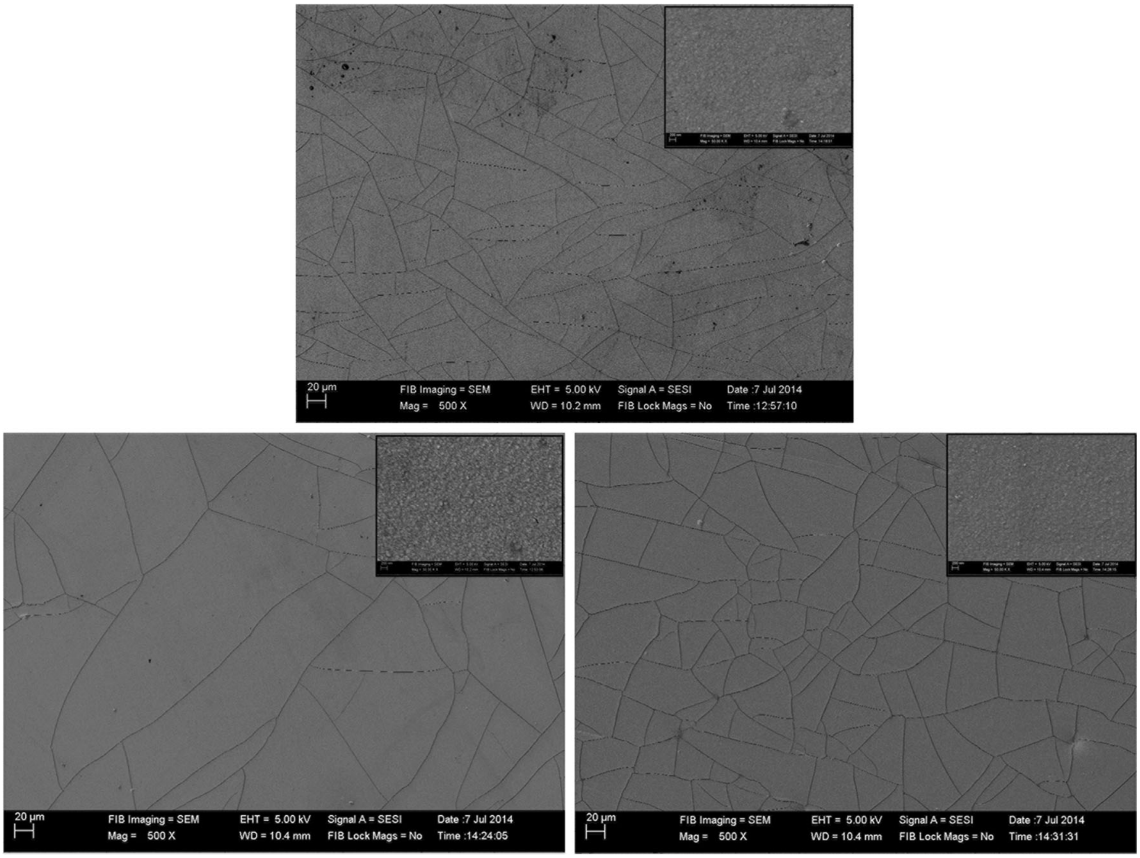

Fig. 2 FESEM images showing microcracks of Ni-W coatings deposited at (a) 2.0 A/dm^2, (b) 3.0 A/dm^2, (c) 4.0 A/dm^2 along with their magnified images in the inset

composition, hardness, and thickness of the coatings, deposited at different c.d.'s are reported in Table 2.

3.2.1 Compositional Analysis. From the data in Table 1, it may be observed that wt.% of W in the deposit increased with c.d. until it reached a maximum of 12.49% at 4.0 A/dm^2 (above this c.d., W content was found to be decreased in the deposit). It is worth noting that despite the high concentration of W in the bath (83.7%), a much lower wt.% of W ($<$12.5%) was found in the deposit. This peculiar behavior of small variation of W content with c.d. may be attributed to the complexation of metal ions, which affected the static potentials of the parent metals markedly (Ref 20). In addition, this unusual change of composition with c.d. is typical of induced codeposition and is a classic example of irregular codeposition, which is explained as follows: Regular codeposition is generally controlled by diffusion of ions toward the cathode film, where the effects of plating variables on the composition of the deposit are determined by changes in the concentrations of metal ions in the cathode diffusion layer (CDL) and are predictable from simple diffusion theory. As explained by Brenner (Ref 4), this irregular codeposition is controlled by the peculiarities of the potentials of the metals against the solution to a greater extent than by diffusion phenomena. The effects of some of the plating variables on the composition of the deposit are in accord with simple diffusion theory and the effects of others are contrary to diffusion theory. Hence, the effects of plating variables on the composition of the deposit are much smaller than with regular alloy plating systems.

3.2.2 Hardness and Thickness. Generally, W-based alloys are of great importance for specific applications due to their unusual properties. Of all the metals, W possesses the highest melting point (3683 K) and highest tensile strength (410 kg/mm^2). This property of the very metal is reflected in the developed alloy too and it is evident by high Vickers micro hardness data reported in Table 2. It may be noted that hardness of the coatings increased with c.d., due to increase of W wt.% in the deposit (Ref 21, 22). In addition, thicker Ni-W alloy coatings were formed toward high c.d., supported by data in Table 2.

3.2.3 Surface Morphology. Surface morphology of the working electrode is one of the important factors in the case of its heterogeneous catalytic activity. In general, an enlarged surface area gives rise to a large number of active sites for reactions. Thus, an increased rate of the hydrogen adsorption and evolution processes can be achieved. The representative FESEM images of Ni-W alloy coatings deposited at 2.0, 3.0, and 4.0 A/dm^2 are shown in Fig. 2. From the images, it may be observed that as c.d. increases the surface morphology of the deposit has changed significantly, indicating that corrosion rate (CR) and catalytic activity of the alloys bear a close relationship with surface morphology. The coatings displayed microcracks with increase in current density, i.e., with increase in tungsten content (Table 2), which is inherent nature of W alloy. As reported by Zhu et al. (Ref 17), the large strains or the microcracks observed on Ni-W coatings were due to hydrogen embrittlement associated with the deposition process. It may explained by the fact that during alloy deposition, hydrogen gas remained adsorbed on the surface due to low hydrogen overvoltage of W. The adsorbed hydrogen leads to the development of strain in the deposit, which subsequently leads to the formation of microcracks on the surface. Thus, microcracks on the surface of coatings may be attributed to low hydrogen overvoltage of W, which was observed to be more at high c.d. The increased surface area due to microcracks, and inherent catalytic property of the deposit is due to high W content, and is responsible for its better catalytic property for HER. Here it should be noted that increased catalytic activity is due to low hydrogen over voltage of W (0.395 mV) compared to that of Ni (0.415 mV) present in the alloy. It was assumed that formation of a layer of mixed tungsten oxides prevents nickel deposition and catalyzes hydrogen evolution.

3.2.4 X-ray Diffraction Study. The phase structures of Ni-W coatings, deposited at different c.d.'s were assessed by XRD analysis. It revealed that the phase structure of the electrodeposited W alloys is different from that of thermally prepared alloys. The identification of the phase structures corresponding to different c.d.'s was obtained from the signals of peak profile of the x-ray reflection, plotted as a function of 2θ. The XRD pattern of Ni-W coatings, deposited at different c.d.'s labeled by their Miller indices is shown in Fig. 3. It may be noted that the intensity of the prominent peak corresponding to the (111) phase increased with c.d., keeping other phases almost constant. From the intensity and reflection angle of XRD signals, it may be seen that c.d. plays an important role on both composition and phase structures of the coatings. The diffractogram shows characteristic peaks of $Ni_{17}W_3$ corresponding to (111) and (200) phases (JCPDS file no. 65-4828) (Ref 23). At higher c.d., a peak corresponding to a new phase with higher W tungsten content in comparison to the $Ni_{17}W_3$ phase as in lower current densities are also visible. The phase corresponds to NiW alloy with (042), (402), and (530) are also found to be present at higher current densities with fcc crystal lattice. The lattice growth from cubic to face-centered cubic increased its crystalline nature and microhardness as evident from the obtained results. Both crystalline $Ni_{17}W_3$ phase and tungsten-rich Ni-W phase are found to be responsible for a decrease of CR and increased catalytic activity of the coatings, deposited at high c.d. Hence by considering this change of composition and phase structure of the Ni-W deposit with deposition c.d., an effort was made to correlate the electrocatalytic behavior with their deposition current densities. The experimental results of investigations are reported in the following sections.

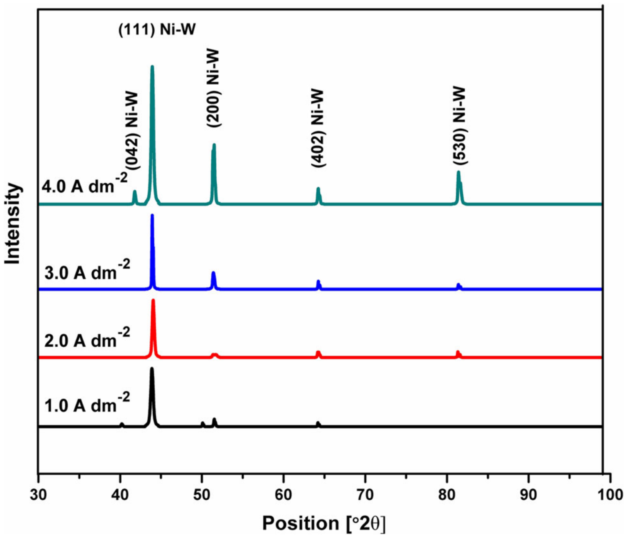

Fig. 3 X-ray diffraction patterns of Ni-W alloy deposited at different c.d.'s from same bath (JCPDS file no. 65-4828)

3.2.5 Corrosion Stability. The corrosion stability of electrocatalytic materials is of great significance as far as their long-term stability in their working condition is concerned. Hence, the stability of electrodeposited Ni-W coatings has been verified by subjecting them to corrosion in 1.0 M KOH (the medium to be used for electrocatalytic study). The corrosion data of deposits corresponding to different c.d.'s were evaluated by Tafel's extrapolation method, and are reported in Table 2. From the data, it may be noted that Ni-W coatings at almost all c.d.'s show reasonably less CR, i.e., in the range from 1.6×10^{-2} to 7.3×10^{-2} mm/year, which are well within the limit of corrosion resistance allowed for electrocatalytic materials (Ref 18). Thus, corrosion data, deduced from polarization study, revealed that electrodeposited Ni-W coatings qualify as efficient electrode materials, with good structural stability for water electrolysis in 1.0 M KOH. It was also found that CR decreased with an increase of c.d. only up to 4.0 A/dm^2, and then increased, which indicates that wt.% W in the deposit bears a close relationship with the corrosion resistance. Hence it may be concluded that Ni-W alloy, deposited at 4.0 A/dm^2 having highest W content (12.5%) was found to be more corrosion resistant compared to all alloys, deposited from the same bath.

Although Tafel polarization data, shown in Table 2, throw some light on electrochemical stability of different Ni-W coatings, they cannot be used for assessing their real ability to HER and OER. This is due to the fact that Tafel curves are normalized to the geometric area of the coatings, and not to the real electrochemical area. Hence the polarization behavior discussed above is either incorrect or does not offer a definite conclusion, if the observed electrocatalytic activity is a result of only an increased surface area of the catalysts, or if an improvement in the intrinsic (electronic) electrocatalytic properties of the catalyst material is also a contributing factor (Ref 24). Therefore, in order to obtain information on the intrinsic activity of the investigated layers in the HER, the curves presented in Fig. 4 should be normalized to the real electrochemically active surface area. Hence, the EIS technique is appropriate to determine the real surface area in electrochemical systems, as previously used in the literature (Ref 25). Accordingly, the impedance data of Ni-W coatings at OCP, corresponding to different c.d.'s are presented in Fig. 5 as Nyquist and Bode representations. The deviation from ideal semicircle was related to the surface in-homogeneities of the coatings (Ref 26). The observation of only one loop in the Nyquist plots indicates that the electrode/electrolyte interfacial reaction is mainly controlled by a charge transfer process (Ref 27). Further, it may be noted that the Nyquist response of impedance for Ni-W deposit at 4.0 A/dm^2 is of maximum radius compared to those at other c.d.'s. It indicates that it offers better electrochemical stability compared to all other deposits. It is further supported by the Bode diagram magnitude plot shown in the inset of Fig. 5.

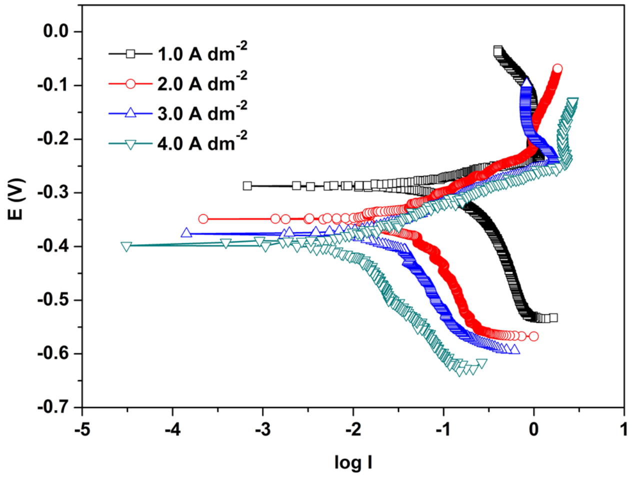

Fig. 4 Potentiodynamic polarization behavior of monolithic Ni-W alloy deposits obtained at different current densities at a scan rate of 1.0 mV/s

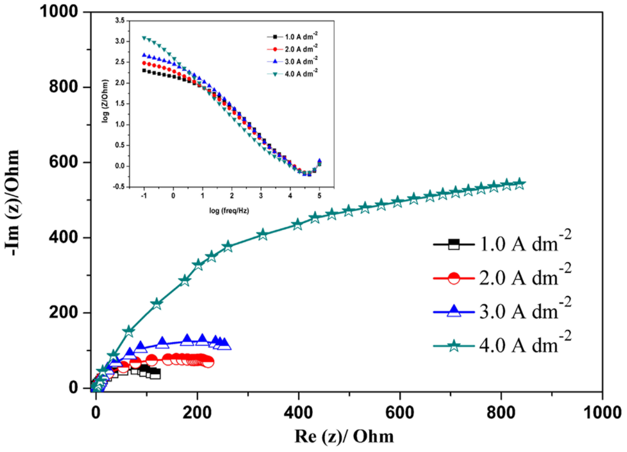

Fig. 5 Nyquist plot of Ni-W alloy deposits obtained at different current densities

3.3 Electrocatalytic Activity for Water Splitting Reaction

The HER and OER on metal and metal-based materials continue to attract great attention among electrochemists. The steady-state equilibrium method is one of the simplest techniques for investigating the electrocatalytic activity in alkaline water electrolysis. Hence Ni-W alloy coatings electrodeposited at different current densities, from the proposed bath, were tested for electrocatalytic activity for HER and OER in 1.0 M KOH, and experimental results are reported as below.

3.3.1 Electrocatalytic Activity for HER. *3.3.1.1 Cyclic Voltammetry Study.* The cyclic voltammetry technique allows determination of a set of parameters that are useful in the evaluation of electrodes. The hydrogen desorption peak area is one of the main parameters among the electrode characteristics. It depends on the active specific surface of the deposit: the larger the active specific surface, the higher the amount of hydrogen produced during the reduction and of the hydrogen adsorbed on the electrode. Another important parameter characterizing cathodic alloys is the discharge potential of hydrogen determining the interception of the voltammetric curve tangent with the *x*-axis. It indicates the electrocatalytic properties of the cathodic material used in the water electrolysis and thus allow evaluation of the energy consumption in hydrogen production (Ref 28). Accordingly, electrocatalytic behaviors of Ni-W alloy deposits for water splitting of both HER and OER have been studied.

The water splitting ability Ni-W alloy coatings for HER has been obtained by cyclic voltammetry (CV) study with a potential ramp of 0.0 to −1.6 V at 50 mV/s scan rate for 50 cycles. The scan rate of 50 mV/s was selected, among different scan rates based on better readability of data. For CV of 50 cycles, the current density peaks at −1.6 V decrease sequentially with increase of number of cycles and then becomes stable. This may be attributed to the progressive resistance induced by the hydrogen bubbles formed on the catalyst surface; and a stable and reproducible CV curves obtained indicated a state of equilibrium between adsorption and desorption of hydrogen gas on the electrode surface (Ref 18). The current density corresponding to stable state of equilibrium for H_2 evolution is called, cathodic peak current density, abbreviated by i_{cp}. Accordingly, CV curves of different Ni-W alloy deposits showing relative i_{cp} are shown in Fig. 6, and

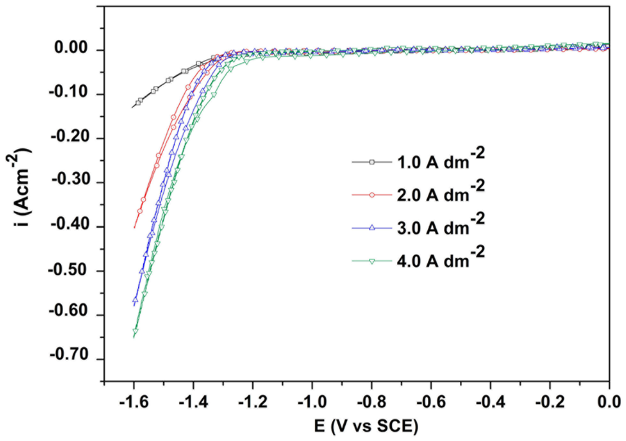

Fig. 6 The CV curves of Ni-W coatings deposited at different c.d.'s demonstrating their cathodic peak current density, i_{cp}

corresponding electrochemical data are given in Table 3. From Fig. 6, it may be noted that the Ni-W coating formed at 4.0 A/dm^2 exhibits the highest i_{cp} (−0.66 A/cm^2), compared to other coatings. Thus the highest i_{cp} values recorded by Ni-W coatings deposited at 4.0 A/dm^2 can be attributed to the highest W content (12.49 wt.%) of the all coatings deposited from the same bath. Further, it may be noted from the data reported in Table 3 that the onset potential for H_2 evolution decreased as the deposition c.d. increased, suggesting that Ni-W coatings deposited at high c.d. are more congenial for HER. Thus, electrocatalytic behavior of Ni-W alloy deposits was found to have a close relationship with the c.d. employed, a dictating parameter of surface morphology, composition, and phase structure of the deposits. Experimental study by Herraiz et al. (Ref 24), demonstrated that the intrinsic catalytic activity for HER on Ni-based electrodeposits depends on the synergism among the catalytic properties of nickel (low hydrogen over potential) and of its counterpart's (high hydrogen adsorption). Hence, it may be concluded that the highest realized i_{cp} value of Ni-W coating corresponding to 4.0 A/dm^2 is attributed to the synergistic effect of lower Ni content (87.5 wt.%) and higher W content (12.5 wt.%) of the deposit.

3.3.1.2 Chronopotentiometry Study. Chronopotentiometry (CP) was used to assess the electrocatalytic behavior of electrodeposited Ni-W alloy coatings, using 1.0 M KOH as electrolyte. The solution is usually, but not necessarily, unstirred and contains an excess of a supporting electrolyte to ensure that mass transport at the electrode/electrolyte interface takes place only through diffusion. The CP study for evolution of hydrogen on Ni-W alloy coatings, deposited at different c.d.'s was made at a constant current density of −300 mA/cm^2 for duration of 1800 s. The electrocatalytic behavior of each coating was evaluated by measuring the amount of H_2 liberated for 300 s. The chronopotentiograms for each Ni-W coatings are shown in Fig. 8, and volume of hydrogen liberated on these coatings for first 300 s is also shown in the inset. It may be noted that Ni-W coating deposited at 4.0 A/dm^2 produced the maximum amount of H_2 gas compared to coatings deposited other c.d.'s This confirmed the fact that Ni-W coating at 4.0 A/dm^2 was the most electrocatalytically active. An initial sharp decrease of potential immediately after starting electrolysis may be observed in some coatings, due to an increased reduction of H^+ to H_2 as the current is applied suddenly. However, the constant potential immediately after a few minutes of starting electrolysis, as in Fig. 7, indicates that HER reaction takes place unabatedly on the electrode surface at applied current density.

Table 3 The hydrogen evolution reaction parameters of Ni-W coatings developed at different c.d.'s from optimal bath

Coating configuration, A/dm^2	Cathodic peak c.d., A cm^{-2}	Onset potential for H_2 evolution (V vs. SCE)	Volume of H_2 evolved in 300 s, cm^3
1.0	−0.11	−1.39	11.1
2.0	−0.42	−1.32	12.2
3.0	−0.58	−1.26	13.4
4.0	−0.66	−1.21	14.8

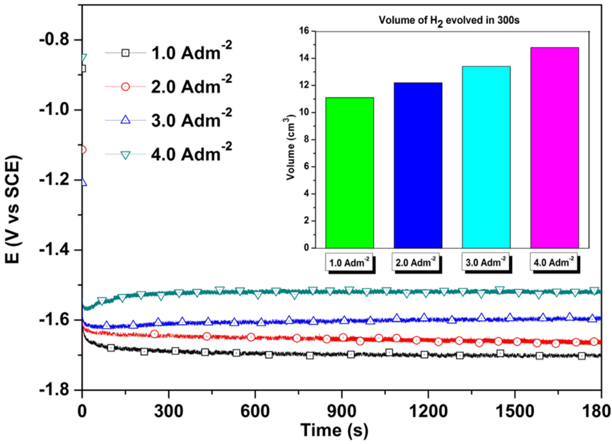

Fig. 7 Chronopotentiometry curves for Ni-W alloy coatings under impressed cathodic current of −300 mA/cm^2, volume of H_2 evolved in 300 s on each test electrodes are shown in the inset

3.3.2 Electrocatalytic Activity for OER. *3.3.2.1 Cyclic Voltammetry Study.* The Ni-W alloy deposited at different c.d.'s was also tested for electrocatalytic activity for OER in 1.0 M KOH, in same line as for HER. The CV experiments for OER on Ni-W alloy deposits were conducted in the potential range of 0 to 0.75 V at a scan rate of 50 mV/s, and corresponding CV's are shown in Fig. 8.

The onset potentials for continuous evolution of O_2 gas for each coatings developed at different c.d.'s are shown in the CV curves. It was observed that the Ni-W alloy deposited at 1.0 A/dm^2 gave good activity toward OER with the lowest onset potential (0.51 V) and maximum anodic peak c.d. at 0.75 V (Fig. 8; Table 4). The mechanism proposed involves the adsorption of OH^- from the medium on to the surface of the electrode followed by the formation of adsorbed oxygen through electron transfer leading to the formation of O_2 gas as shown in Fig. 10(b) (Ref 29, 30).

The cathodic and an anodic peaks observed in cyclic voltammograms (Fig. 10) in the applied potential range (0.0 to +0.75 V) are due to the formation and reduction of a NiOOH layer. In this potential range, the substrate surface is covered with a thin p-type semiconducting layer of NiO(H_2O) (Ref 31), and can enhance the OER within the potential range by

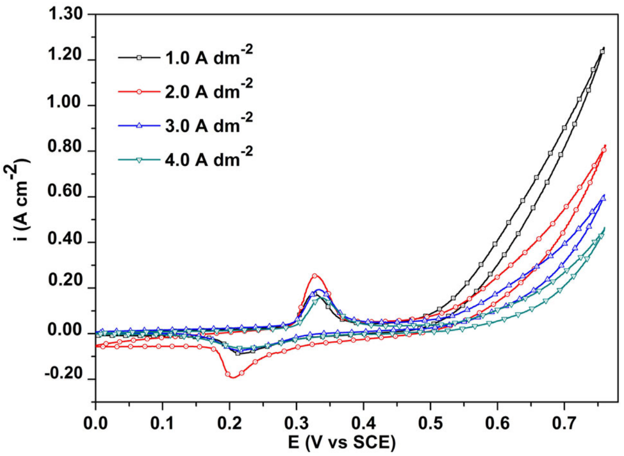

Fig. 8 CV curves for OER studies of Ni-W alloys deposited at different c.d.'s

enhancing the OH^- adsorption. While apart from this potential range, the activity will be limited due to the lack of formation of semiconducting layer of $NiO(H_2O)$. This is in agreement with the well-established generalization on OER; that it normally takes place on a metal surface which is firstly covered with appropriate oxides (Ref 32). In the present study, the coating developed at 1.0 A/dm^2 shows maximum activity toward OER due to its higher Ni content leading to better adsorption of OH^- through redox reaction under the applied potential.

3.3.2.2 Chronopotentiometry Studies. The efficiency of electroactive coatings of Ni-W alloy for OER has also been tested using chronopotentiometry. The amount of oxygen evolved was measured in the similar way as discussed earlier, and corresponding chronopotentiograms are shown in Fig. 9. As the current pulse of +300 mA/cm^2 was applied, a sharp increase in the potential was observed until a potential at which OH^- is oxidized to O_2 is reached. In other words, an equilibrium state is reached between newly forming bubble and bubbles escaping from the surface of the electrode (Ref 18, 24). The inset in Fig. 9 shows the relative amount of O_2 liberated in 300 s on Ni-W coatings deposited at different c.d.'s, and corresponding volumes are given in Table 4. In this case, the amount of O_2 liberated on the surface coating formed at 4.0 A/dm^2 is less compared to other coatings. In other words, the Ni-W alloy deposited at 1.0 A/dm^2 exhibits the lowest potential for O_2 evolution. Hence, the Ni-W alloy coating deposited at 1.0 A/dm^2 is more electroactive for OER compared to other coatings. Thus, from experimental results of HER and OER of electrodeposited Ni-W alloy coatings deposited at different c.d.'s, it may be inferred that the surface favoring the cathodic reaction has an adverse effect on anodic reaction and vice versa. It may be due to unique phase structure and composition of the coatings deposited at different c.d.'s, but from the same bath. To sum up, an increase of H_2 and O_2 evolution with c.d., is found as shown in Fig. 7 and 9, respectively. This indicates a synergism between the good catalytic property of W (due to low hydrogen overvoltage) and Ni (having increased adsorption of OH^- ions) for better catalytic properties of the Ni-W deposit as cathode and anode, respectively.

Table 4 The OER parameters of Ni-W coatings electrodeposited at different c.d.'s

Coating configuration, A/dm^2	Anodic peak c.d. at 0.75 V, A/cm^2	Onset potential of O_2 evolution (V vs. SCE)	Volume of O_2 evolved in 300 s, cm^3
1.0	1.25	0.51	13.1
2.0	0.83	0.53	12.6
3.0	0.61	0.57	11.8
4.0	0.45	0.61	11.1

3.3.2.3 Mechanism of HER and OER. The factors responsible for increased HER and OER on Ni-W electrodes deposited, respectively, at 4.0 and 1.0 A/dm^2 can be explained by a mechanism as shown in Fig. 10. The schematic representation of the steps such as chemisorption, desorption, and recombination leading to the evolution of H_2 gas on Ni-W electrode surface is given in Fig. 10(a). The physical properties of the coatings like size, shape, composition, and crystallographic structure are equally responsible for their catalytic activity toward HER. High-catalytic efficiency of Ni-W alloy, deposited at 4.0 A/dm^2 may be attributed to an increased W content (12.49 wt.%) of the alloy. The increase of W (having low hydrogen overvoltage) leads to promotion of the evolution of hydrogen. In addition, properties like increased surface area, due to microcracks also contribute to more H^+ adsorption and hence catalytic activity.

Contrarily, the Ni-W alloy deposited at low c.d. (having low wt.% of W) was found to be more efficient electrode material, when it is used as anode, i.e., for OER reaction. The mechanism of OER on Ni-W alloy, when used as anode, is shown schematically in Fig. 10(b). This behavior may be explained by the adsorption of comparatively large OH^- ions on electrode surface, where it overlaps with other processes like oxygen reduction reaction at the same time. Thus, enhanced OER activity of Ni-W coating, developed at 1.0 A/dm^2 can be attributed to the increased OH^- adsorption through the formation of a semiconducting layer in the applied potential range.

Since the adsorption characteristics of the OH^- can lead to the formation of NiOOH on its surface, the increase of Ni content in the coating (98.5%), deposited at 1.0 A/dm^2 largely

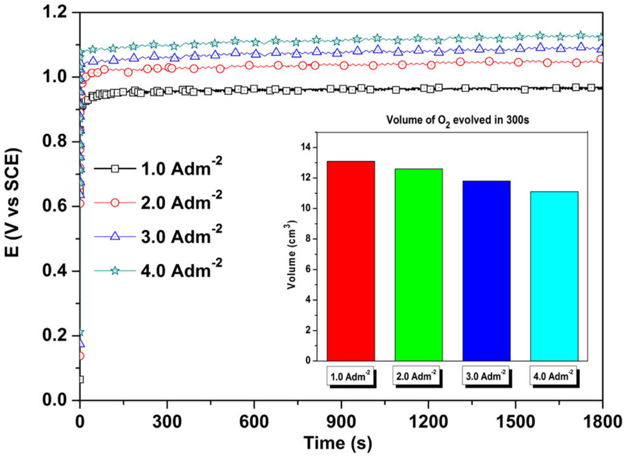

Fig. 9 Chronopotentiograms for Ni-W alloy coatings under impressed anodic current of +300 mA/cm^2, volume of O_2 evolved in 300 s on each test electrodes are shown in the inset

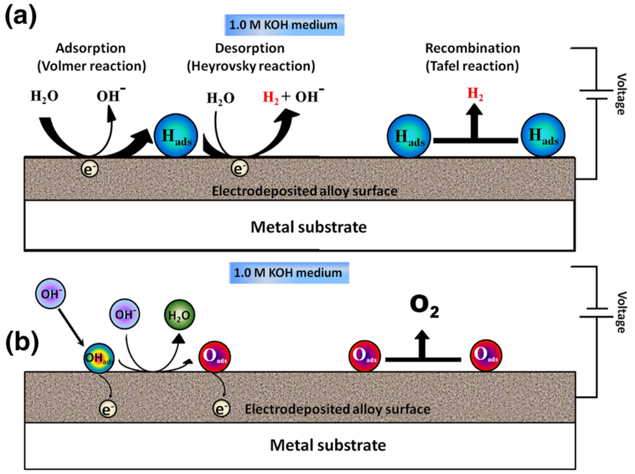

Fig. 10 Mechanism of electrocatalytic (a) hydrogen evolution (HER) and (b) oxygen evolution reaction (OER)

favors the OER. As the Ni content in the coating decreases, the oxide layer formation will become limited and thereby reduces OER. Therefore, it may summarize that the Ni-W electrode material favoring HER has an adverse effect on OER and vice versa.

4. Conclusions

In this study, Ni-W alloy coatings have been developed through a compositionally versatile electrodeposition method from a new tri-sodium citrate bath, using glycerol as the additive. Deposits with various chemical compositions were synthesized on copper, and their possible applications as electrocatalytic materials for water splitting (HER and OER) have been tested by CV and CP methods. All Ni-W coatings were found to be stable in the working conditions of its electrocatalytic study confirmed by potentiodynamic polarization and EIS study. The effects of c.d. on deposit characteristics, as function of their electrocatalytic efficiency for HER and OER, have been tested using CV and CP studies. It was found that Ni-W alloy deposited, respectively, at 4.0 A/dm^2 (having about 12.49 wt.% W) and 1.0 A/dm^2 (having about 0.95 wt.% W) is good electrode materials for HER and anode for OER, deposited from the same bath. It was observed that Ni-W alloy favoring HER has an adverse effect on OER and vice versa. This is due to the presence of some reactive sites, which responds to the process, based on situation whether it is used as a cathode or anode. An increase in H_2 and O_2 evolution with c.d. was found, and it indicates the existence of a synergism between high-catalytic property of W (due to low hydrogen overvoltage) and Ni (having increased adsorption of OH^- ions) for better catalytic property of Ni-W deposit as cathode and anode, respectively. A synergism between high-catalytic property of W, having low hydrogen overvoltage and of Ni, caused by increased adsorption of OH^- ions (depending on the composition of the alloy) was found, and is responsible for the better catalytic property of the deposit, both as cathode and anode. The FESEM, EDS, and XRD studies supported the fact that Ni-W alloy deposit, developed at different c.d.'s, has specific electrocatalytic activity, influenced by their composition, surface morphology, and phase structures.

Acknowledgments

Liju Elias is thankful to NITK, Surathkal, India for supporting this research in the form of Institute Research Fellowship. Authors are thankful to Department of Met. and Mat. Eng. NITK, Surathkal for extending XRD, FESEM, and EDS facility for analyses.

References

1. G. Lu and G. Zangari, Study of the Electroless Deposition Process of Ni-P-Based Ternary Alloys, *J. Electrochem. Soc.*, 2003, **150**(11), p C777–C786
2. H. Hosokawa, T. Yamasaki, N. Sugamoto, M. Tomizawa, K. Shimojima, and M. Mabuchi, Bending Properties of Nanocrystalline Ni-18 at.% W Alloy Produced by Electrodeposition, *Mater. Trans.*, 2004, **45**(5), p 1807–1810
3. T.M. Sridhar, N. Eliaz, and E. Gileadi, Electroplating of Ni4W, *Electrochem. Solid State Lett.*, 2005, **8**(3), p C58–C61
4. A. Brenner, *Electrodeposition of Alloys: Principles and Practice*, Academic Press, New York, 1963
5. N. Eliaz and E. Gileadi, Induced Codeposition of Alloys of Tungsten, Molybdenum and Rhenium with Transition Metals, *Modern Aspects of Electrochemistry*, C.G. Vayenas, R.E. White, and M.E. Gamboa-Aldeco, Ed., Springer, New York, 2008, p 191–301
6. N.V. Krstajić, V.D. Jović, L. Gajić-Krstajić, B.M. Jović, A.L. Antozzi, and G.N. Martelli, Electrodeposition of Ni-Mo Alloy Coatings and Their Characterization as Cathodes for Hydrogen Evolution in Sodium Hydroxide Solution, *Int. J. Hydrogen Energy*, 2008, **33**(14), p 3676–3687
7. J.R. McKone, E.L. Warren, M.J. Bierman, S.W. Boettcher, B.S. Brunschwig, N.S. Lewis, and H.B. Gray, Evaluation of Pt, Ni, and Ni-Mo Electrocatalysts for Hydrogen Evolution on Crystalline Si Electrodes, *Energy Environ. Sci.*, 2011, **4**(9), p 3573–3583
8. H. Ataee-Esfahani, L. Wang, Y. Nemoto, and Y. Yamauchi, Synthesis of Bimetallic Au@ Pt Nanoparticles with Au Core and Nanostructured Pt Shell Toward Highly Active Electrocatalysts, *Chem. Mater.*, 2010, **22**(23), p 6310–6318
9. H. Wang, S. Ishihara, K. Ariga, and Y. Yamauchi, All-Metal Layer-by-Layer Films: Bimetallic Alternate Layers with Accessible Mesopores for Enhanced Electrocatalysis, *J. Am. Chem. Soc.*, 2012, **134**(26), p 10819–10821
10. T.-L. Wee, B.D. Sherman, D. Gust, A.L. Moore, T.A. Moore, Y. Liu, and J.C. Scaiano, Photochemical Synthesis of a Water Oxidation Catalyst Based on Cobalt Nanostructures, *J. Am. Chem. Soc.*, 2011, **133**(42), p 16742–16745
11. I.J. Godwin and M.E.G. Lyons, Enhanced Oxygen Evolution at Hydrous Nickel Oxide Electrodes via Electrochemical Ageing in Alkaline Solution, *Electrochem. Commun.*, 2013, **32**, p 39–42
12. M. Gong, Y. Li, H. Wang, Y. Liang, J.Z. Wu, J. Zhou, J. Wang, T. Regier, F. Wei, and H. Dai, An Advanced Ni-Fe Layered Double Hydroxide Electrocatalyst for Water Oxidation, *J. Am. Chem. Soc.*, 2013, **135**(23), p 8452–8455
13. T. Takashima, K. Hashimoto, and R. Nakamura, Inhibition of Charge Disproportionation of MnO_2 Electrocatalysts for Efficient Water Oxidation Under Neutral Conditions, *J. Am. Chem. Soc.*, 2012, **134**(44), p 18153–18156
14. X. Li, F.C. Walsh, and D. Pletcher, Nickel Based Electrocatalysts for Oxygen Evolution in High Current Density, Alkaline Water Electrolysers, *PCCP*, 2011, **13**(3), p 1162–1167
15. R.D. Smith, M.S. Prévot, R.D. Fagan, S. Trudel, and C.P. Berlinguette, Water Oxidation Catalysis: Electrocatalytic Response to Metal Stoichiometry in Amorphous Metal Oxide Films Containing Iron, Cobalt, and Nickel, *J. Am. Chem. Soc.*, 2013, **135**(31), p 11580–11586
16. S. Nagalingam, G.B. Teh, R.-F. Louh, and K.T. Chee, Cyclic Voltammetry Studies of Cadmium Zinc Sulfide Aqueous Solution, *Int. J. Phys. Sci.*, 2011, **6**(31), p 7166–7170
17. L. Zhu, O. Younes, N. Ashkenasy, Y. Shacham-Diamand, and E. Gileadi, STM/AFM Studies of the Evolution of Morphology of Electroplated Ni/W Alloys, *Appl. Surf. Sci.*, 2002, **200**(1–4), p 1–14
18. Y. Ullal and A.C. Hegde, Electrodeposition and Electro-catalytic Study of Nanocrystalline Ni-Fe Alloy, *Int. J. Hydrogen Energy*, 2014, **39**(20), p 10485–10492
19. N. Parthasaradhy, *Practical Electroplating Handbook (Retroactive Coverage)*, Prentice-Hall, Inc., Upper Saddle River, 1996, p 1444–1989
20. M. Bratoeva and N. Atanasov, Effect of Sulfamate-Citrate Electrolyte pH on the Ni-W Alloy Electrodeposition, *Russ. J. Electrochem.*, 2000, **36**(1), p 60–63
21. Z.S. Ma, Y.C. Zhou, S.G. Long, and C. Lu, On the Intrinsic Hardness of a Metallic Film/Substrate System: Indentation Size and Substrate Effects, *Int. J. Plast*, 2012, **34**, p 1–11
22. Z. Ma, S. Long, Y. Pan, and Y. Zhou, Indentation Depth Dependence of the Mechanical Strength of Ni Films, *J. Appl. Phys.*, 2008, **103**(4), p 043512
23. M. Zemanová, R. Kurinec, V. Jorík, and M. Kadlečíová, Ni-W Alloy Coatings Deposited from a Citrate Electrolyte, *Chem. Pap.*, 2012, **66**(5), p 492–501

24. I. Herraiz-Cardona, E. Ortega, J.G. Antón, and V. Pérez-Herranz, Assessment of the Roughness Factor Effect and the Intrinsic Catalytic Activity for Hydrogen Evolution Reaction on Ni-Based Electrodeposits, *Int. J. Hydrogen Energy*, 2011, **36**(16), p 9428–9438
25. A. Kellenberger, N. Vaszilcsin, W. Brandl, and N. Duteanu, Kinetics of Hydrogen Evolution Reaction on Skeleton Nickel and Nickel-Titanium Electrodes Obtained by Thermal arc Spraying Technique, *Int. J. Hydrogen Energy*, 2007, **32**(15), p 3258–3265
26. F. Rosalbino, D. Maccio, E. Angelini, A. Saccone, and S. Delfino, Electrocatalytic Properties of Fe-R (R = Rare Earth Metal) Crystalline Alloys as Hydrogen Electrodes in Alkaline Water Electrolysis, *J. Alloys Compd.*, 2005, **403**(1), p 275–282
27. E. Navarro-Flores, Z. Chong, and S. Omanovic, Characterization of Ni, NiMo, NiW and NiFe Electroactive Coatings as Electrocatalysts for Hydrogen Evolution in an Acidic Medium, *J. Mol. Catal. A*, 2005, **226**(2), p 179–197
28. C. Lupi, A. Dell'Era, and M. Pasquali, Nickel-Cobalt Electrodeposited Alloys for Hydrogen Evolution in Alkaline Media, *Int. J. Hydrogen Energy*, 2009, **34**(5), p 2101–2106
29. M.E. Lyons, The Oxygen Evolution Reaction on Passive Oxide Covered Transition Metal Electrodes in Aqueous Alkaline Solution. Part 1—Nickel, *Int. J. Electrochem. Sci.*, 2008, **3**, p 1386–1424
30. K. Jüttner, Oxygen reduction Electrocatalysis by Underpotential Deposited Metal Atoms at Different Single Crystal Faces of Gold and Silver, *Electrochim. Acta*, 1984, **29**(11), p 1597–1604
31. P. Peeters, G.V.D. Hoorn, T. Daenen, A. Kurowski, and G. Staikov, Properties of Electroless and Electroplated Ni-P and Its Application in Microgalvanics, *Electrochim. Acta*, 2001, **47**(1), p 161–169
32. J. Kubisztal and A. Budniok, Study of the Oxygen Evolution Reaction on Nickel-Based Composite Coatings in Alkaline Media, *Int. J. Hydrogen Energy*, 2008, **33**(17), p 4488–4494